

# Constraining Dark Energy Equation of State with Cosmic Voids

Jounghun Lee\* and Daeseong Park

Department of Physics and Astronomy, FPRD, Seoul National University, Seoul 151-747, Korea

Our universe is observed to be accelerating due to the dominant dark energy with negative pressure. The dark energy equation of state ( $w$ ) holds a key to understanding the ultimate fate of the universe. Assuming a flat universe and priors on the matter density parameter ( $\Omega_m$ ) and the Hubble parameter ( $h$ ), we show for the first time that the ellipticity evolution of cosmic voids can provide a robust constraint on the dark energy equation of state.

PACS numbers: 98.65.Dx, 95.75.-z, 98.80.Es

*Introduction.*—Recent observations have revealed that our universe is flat and in a phase of acceleration [1]. It implies that some mysterious dark energy fills dominantly the universe at present epoch, exerting anti-gravity. The nature of this mysterious dark energy which holds a key to understanding the ultimate fate of the universe is often specified by its equation of state, i.e., the ratio of its pressure to density:  $w \equiv P_{de}/\rho_{de}$ . It is now the most challenging task in modern cosmology to measure the value of this  $w$  parameter.

The anti-gravity of the dark energy corresponds to the negative value of  $w$ . The simplest candidate for the dark energy is the vacuum energy or cosmological constant ( $\Lambda$ ) with  $w = -1$  which is constant at all times [2]. Although all current data are consistent with the vacuum energy model [3], the notorious failure of the theoretical estimate of  $\rho_\Lambda$  [4] has led a new class of dark energy to emerge as an alternative. In this alternative model which is often called quintessence, the dark energy is described as a slowly rolling scalar field with  $-1 < w < 0$  [5].

So far, the dark energy equation of state has been probed by utilizing the evolution of cluster abundance [6], the baryonic oscillations in the galaxy power spectrum [7], and the weak gravitational lensing effect [8]. While these previous probes have been found to be useful, it is still quite important to develop as many independent probes as possible for complimentary tests.

In this Letter we investigate the ellipticity evolution of cosmic voids by extending the analytic model developed in our previous work [9] to higher redshifts and explore the possibility of using it as a new complimentary probe of the dark energy equation of state.

*Evolution of the Void Ellipticity*— The tidal forces from the surrounding matter induce ellipticity in the spatial distributions of void halos (or galaxies). Due to the low density, the void regions are more vulnerable to the tidal effect [10].

According to our previous work [9], the ellipticity of a void region can be quantified in terms of the eigenvalues of the local tidal shear tensor. The formula that relates

the void ellipticity to the tidal field starts with

$$\lambda_1(\mu, \nu) = \frac{1 + (\delta_v - 2)\nu^2 + \mu^2}{(\mu^2 + \nu^2 + 1)}, \quad (1)$$

$$\lambda_2(\mu, \nu) = \frac{1 + (\delta_v - 2)\mu^2 + \nu^2}{(\mu^2 + \nu^2 + 1)}, \quad (2)$$

where  $\{\lambda_i\}_{i=1}^3$  (with  $\lambda_1 > \lambda_2 > \lambda_3$ ) are the three eigenvalues of the local tidal tensor defined at the void region,  $\delta_v$  is the critical linear density contrast of a void, which equals the sum of the three eigenvalues:  $\delta_v = \sum_{i=1}^3 \lambda_i$ , and  $\{\mu, \nu\}$  (with  $\nu < \mu$ ) are the two axial ratios of a given void region. The void ellipticity as  $\epsilon \equiv 1 - \nu$ .

The joint probability distribution of  $\mu$  and  $\nu$  was derived as

$$\begin{aligned} p[\mu, \nu; \sigma(R_L)] &= \frac{3375\sqrt{2}}{\sqrt{10\pi}\sigma^5(R_L)} \exp\left[-\frac{5\delta_v^2}{2\sigma^2(R_L)} + \frac{15\delta_v(\lambda_1 + \lambda_2)}{2\sigma^2(R_L)}\right] \\ &\times \exp\left[-\frac{15(\lambda_1^2 + \lambda_1\lambda_2 + \lambda_2^2)}{2\sigma^2(R_L)}\right] (2\lambda_1 + \lambda_2 - \delta_v) \\ &\times (\lambda_1 - \lambda_2)(\lambda_1 + 2\lambda_2 - \delta_v) \frac{4(\delta_v - 3)^2\mu\nu}{(\mu^2 + \nu^2 + 1)^3}. \end{aligned} \quad (3)$$

Then, the void ellipticity was evaluated as

$$p(1 - \epsilon) = p(\nu; R_L) = \int_\nu^1 p[\mu, \nu | \delta = \delta_v; \sigma(R_L)] d\mu. \quad (4)$$

Here,  $\sigma(R_L)$  is the linear rms fluctuation of the matter density field smoothed on a Lagrangian void scale of  $R_L$ :

$$\sigma^2(R_L) \equiv \int_{-\infty}^{\infty} \Delta^2(k) W^2(kR_L) d\ln k, \quad (5)$$

where  $W(kR_L)$  is a top-hat window function, and  $\Delta^2(k)$  is the dimensionless linear power spectrum. Throughout this study, we assume that the linear power spectrum  $\Delta^2(k)$  does not depend on the value of  $w$ .

The above analytic model was originally derived for the present epoch ( $z = 0$ ). Extension of this model to higher redshifts ( $z > 0$ ) can be done by replacing  $\sigma(R_L)$  in Eq. [4] by  $\sigma(z, R_L)$ , which is defined as

$$\sigma^2(z, R_L) \equiv D^2(z)\sigma^2(R_L). \quad (6)$$

\*Electronic address: jounghun@astro.snu.ac.kr

TABLE I: The mean effective radius ( $\bar{R}_E$ ), the corresponding Lagrangian radius ( $\bar{R}_L$ ), the mean density ( $\bar{\delta}_v$ ), the total number of voids ( $N_v$ ) at  $z = 0, 0.5$  and  $1$ .

$z$	$\bar{R}_E$	$\bar{R}_L$	$\bar{\delta}_v$	$N_v$
0	$9.51 \pm 1.73$	$4.41 \pm 0.80$	$0.9 \pm 0.03$	28001
0.5	$9.42 \pm 1.66$	$2.91 \pm 0.51$	$0.9 \pm 0.03$	26772
1	$9.39 \pm 1.62$	$2.17 \pm 0.37$	$0.89 \pm 0.03$	25973

Here the linear growth factor,  $D(z)$ , represents the growth rate of matter fluctuations, depending sensitively on the dark energy equation of state as [11]

$$D(z) \equiv \frac{2\Omega_m E(z)}{2} \int_z^\infty \frac{(1+z')}{E^3(z')} dz', \quad (7)$$

with

$$E(z) = [\Omega_m(1+z)^3 + \Omega_{de}(1+z)^\beta]^{1/2}, \quad (8)$$

where  $\beta \equiv 3(1+w)$  and  $\Omega_{de}$  is the density parameter of the dark energy. For a flat universe, it satisfies the constraint of  $\Omega_m + \Omega_{de} = 1$ . According to Eq. [1]-[8], the void ellipticity distribution is exponentially sensitive to the linear growth factor,  $D(z)$ , which in turn depends strongly on the value of  $w$ .

Before quantifying the dependence of the void ellipticity evolution on the value of  $w$ , however, we perform a numerical test of the analytic model to check its validity at high redshifts. We analyze the  $z = 0, 0.5$  and  $1$  catalogs from the Millennium Run simulation, adopting a  $\Lambda$ CDM cosmology with the key parameters given as  $\Omega_m = 0.25$ ,  $n_s = 1$ ,  $\sigma_8 = 0.9$  and  $h = 0.73$  [13]. We identify voids in each halo catalog with the help of the Hoyle-Vogeley void finder algorithm [14]. Selecting only those voids which contain more than five halos, we calculate the inertia momentum tensors using the positions of the void halos in the center of mass frame. Then, we determine the ellipticity of each void from the eigenvalues of the inertia momentum tensor [9]. For a more detailed description of the void finder algorithm and the measurement of the void ellipticity, see our previous work [9].

The mean effective Eulerian radius ( $R_E$ ), the mean Lagrangian radius ( $R_L$ ), the mean density contrast ( $\delta_v$ ), and the total number of voids ( $N_v$ ) found at three redshifts are listed in Table I. In each column, the errors represent one standard deviation. The *effective* Eulerian radius of a void is defined as  $R_E \equiv (3\Gamma_V/4\pi)^{1/3}$  where  $\Gamma_V$  is a void volume estimated by means of the Monte-Carlo integration method suggested by [14]. According to the mass-conservation law, the corresponding Lagrangian radius is found as

$$\bar{R}_L = \frac{1}{1+z} (1+\delta_v)^{1/3} \bar{R}_E. \quad (9)$$

To compare the analytic model (Eq. [4]) with the numerical result at each redshift, we use the mean Lagrangian radius,  $\bar{R}_L$ , listed in Table I as a smoothing void scale for the calculation of  $\sigma(R_L)$  in Eq. [5]. And we adopt the approximation formula for the dimensionless power spectrum  $\Delta^2(k)$  given by [12] with the shape parameter  $\Gamma \equiv \Omega_m h$ .

Fig. 1 plots the void ellipticity distribution at  $z = 0, 0.5$  and  $1$  in the left, middle, and right panel, respectively. In each panel, the histogram with Poisson errors and the solid line represent the numerical and the analytic result, respectively. As can be seen, the analytic predictions agree with the numerical results excellently at all three redshifts, which proves the validity of our model at higher redshifts.

Apparently, the void ellipticity distribution seems not to change significantly with redshift, according to the results shown in Fig. 1. However, note that we use different Lagrangian smoothing scales  $R_L$  at different redshifts (see Table I) to compute the void ellipticity distribution. In other words, the results shown in the three panels of Fig. 1 represent the ellipticity distributions of voids whose Lagrangian sizes are all different. If we considered the same void scale at the three redshifts, then the ellipticity distribution would change sensitively with redshift.

Just as the cluster mass is fixed when the abundance evolution of clusters is investigated, it should be necessary to set the Lagrangian radius of a void at a certain scale to examine the ellipticity evolution of voids. In practice, it corresponds to increasing the mean effective radius of voids,  $R_E$ , with redshifts. Setting the Lagrangian void scale  $R_L$  at  $4h^{-1}$  Mpc which corresponds to  $R_E = 8.5h^{-1}$  at present epoch (see Eq. [9]), we evaluate the void ellipticity distribution at  $z = 0, 0.5$  and  $1$  for the case of a flat  $\Lambda$ CDM cosmology. Fig. 1 shows how the void ellipticity distribution changes with redshift. The solid, dashed, and dotted lines represent the void ellipticity distribution at  $z = 0, 1$  and  $2$ , respectively. As can be seen, the void ellipticity moves to the low ellipticity section as the redshift increases.

Now that we have seen the ellipticity evolution of voids for the case of  $w = -1$ , we would like to explore how the rate of the decrease changes with the value of  $w$ . Using Eq. [1]-[8], we evaluate the mean ellipticity of voids as a function of  $z$  as

$$\bar{\varepsilon}(z) = \int_0^1 \varepsilon p(\varepsilon; R_L, z). \quad (10)$$

for different values of  $w$  through Eq. [3]-[8]. The key cosmological parameters other than  $w$  are assumed to be given as priors by a fiducial model. Here, we use the values as a fiducial model with which the Millennium Run halo catalogs are constructed. Fig. 3 plots the mean void ellipticities versus redshift for the four different cases of the  $w$  parameter:  $w = -1, -2/3, -1/3$  and  $-1/6$  (solid, dashed, dotted, and dot-dashed line, respectively). As

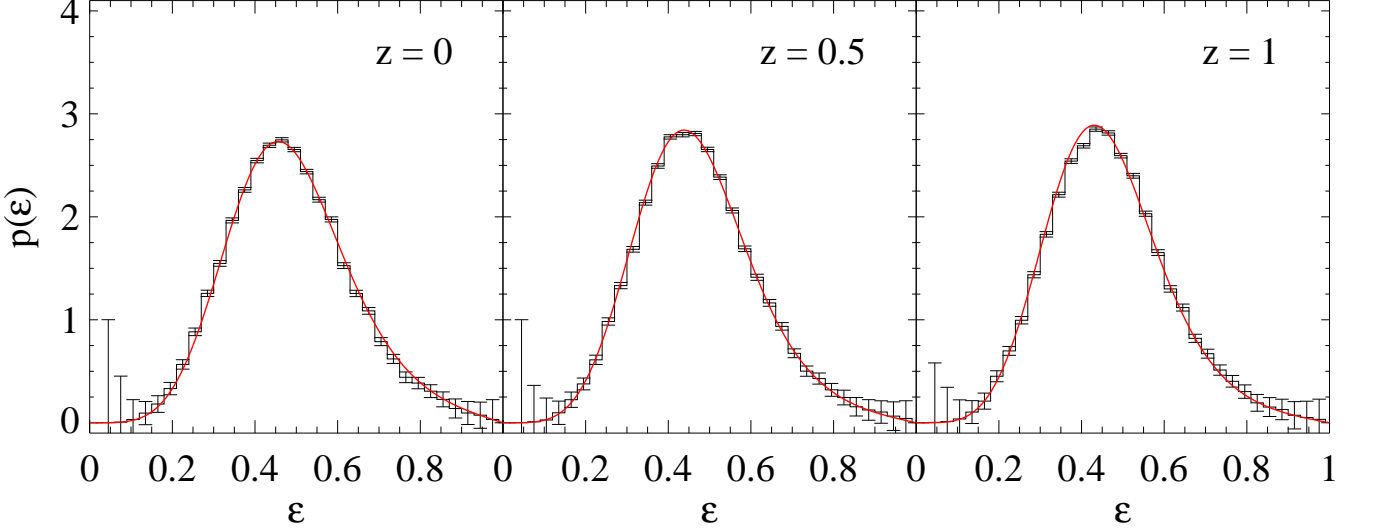


FIG. 1: Probability density distributions of the void ellipticity at three different redshifts:  $z = 0, 1$ , and  $2$  in the left, middle and right panels, respectively. The solid line represents the analytic prediction while the histogram with Poisson error corresponds to the numerical results from the Millennium Run simulation.

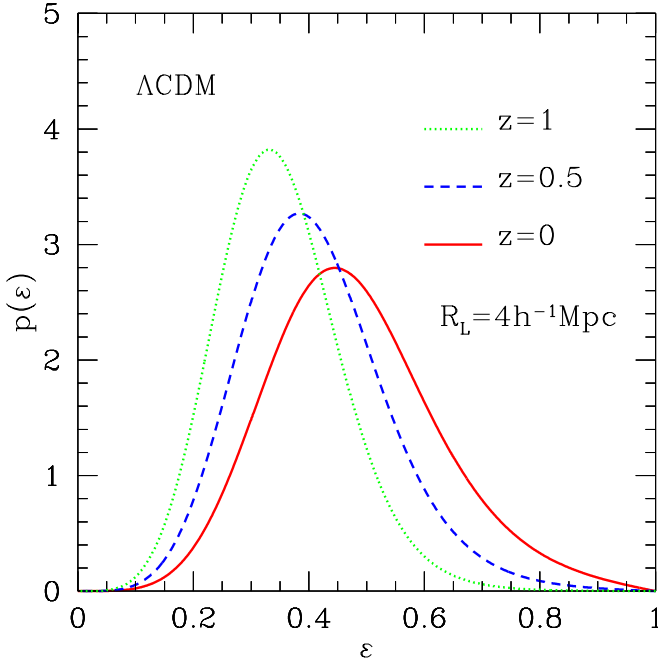


FIG. 2: Probability density distribution of  $\varepsilon_4$  at redshifts  $z = 0, 0.5$  and  $1$  for a  $\Lambda$ CDM cosmology.

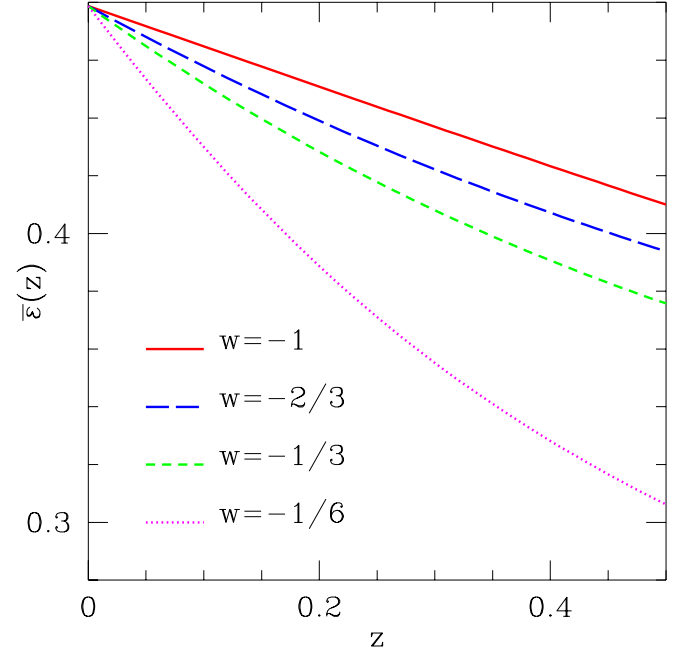


FIG. 3: Mean ellipticity of the voids with size of  $8h^{-1}\text{Mpc}$  as a function of the redshift for three different cases of the dark energy equation of state  $w$ . For each case, the void Lagrangian radius is set at  $4h^{-1}\text{Mpc}$ .

can be seen, the rate of the decrease of the mean void ellipticity with redshift depends strongly on the values of  $w$ . The lower the absolute value of  $w$  is, the higher the rate of the ellipticity decrease is. Fig. 10 also indicates that in the low redshift range of  $0 \leq z \leq 0.2$ , the mean void ellipticity  $\varepsilon(z)$  is well approximated as a linear

function of  $z$ . We fit  $\varepsilon(z)$  to a straight line as

$$\varepsilon(z) \approx A_v z + B_v. \quad (11)$$

Varying the value of  $w$ , we examine how the best-fit slope  $A_v$  changes. Fig. 4 plots  $A_v$  as a function of  $w$ . It shows

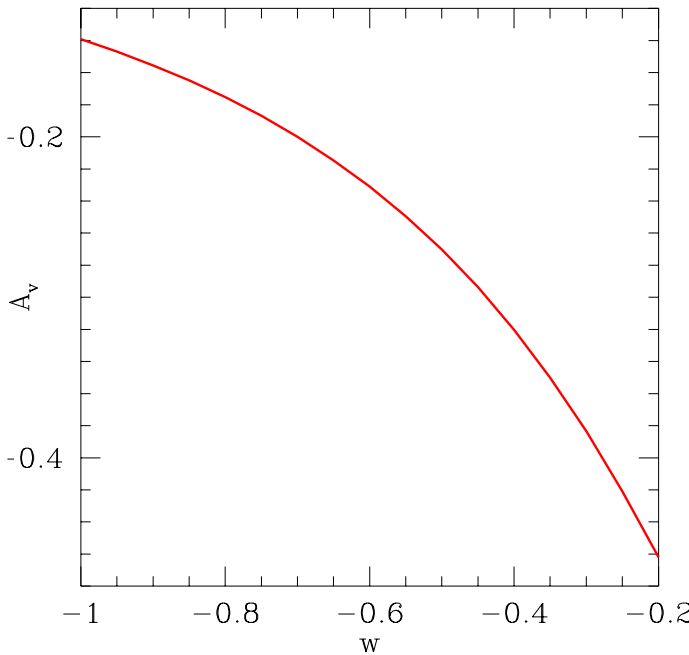


FIG. 4: Slope of the dependence of the void ellipticity on the redshift as a function of the dark energy equation of state.

clearly that the slope, i.e., the rate of the ellipticity evolution of voids in the range of  $0 < z < 0.2$  decreases noticeably as the absolute value of  $w$  increases. A crucial implication of this result is that by measuring the ellipticity evolution of voids in the relatively low redshift, we can place a robust constraint on the value of  $w$ . . *Discussion.*—We have presented a proof of concept that the ellipticity evolution of cosmic voids can place a robust constraint on the dark energy equation of state. The analytic model for the void ellipticity distribution that our probe is based on has successfully survived numerical tests at high redshifts. Furthermore, the model is completely described by linear physics alone, which makes our method optimal for the dark energy probe.

This new dark energy probe with cosmic voids is unique and independent, so that it can compliment the previous methods. It deals with only measuring the ellipticity of voids using the positions of void galaxies (or halos). Thus, it can be readily applied to the real observational data. As the void catalogs from large galaxy surveys like the Sloan Digital Sky Survey [15] is coming on line soon and the the precise measurements of the key cosmological parameters are expected from *Planck* mission, this new dark energy probe with cosmic voids might play a crucial role in unveiling the mystery of dark energy.

The Millennium Run simulation used in this paper was carried out by the Virgo Supercomputing Consortium at the Computing Centre of the Max-Planck Soci-

ety in Garching. We thank G. Lemson and V. Springel for useful comments. This work is supported by the research grant No. R01-2005-000-10610-0 from the Basic Research Program of the Korea Science and Engineering Foundation.

---

- [1] A. G. Riess *et al.*, Astron. J. **116**, 1009 (1998); S. Perlmutter *et al.*, Astrophys. J. **517**, 565 (1999); D. N. Spergel *et al.*, Astrophys. J. Supp. **148**, 175 (2003)
- [2] A. Einstein, Sitz. Preuss. Akad. Wiss. **142**, (1917)
- [3] Y. Wang, and M. Tegmark, Phys. Rev. Lett. **92**, 241302 (2004); H. K. Jassal, J. S. Bagla, and T. Padmanabhan, Mon. Not. R. Astron. Soc. **356** L11 (2005)
- [4] S. M. Carroll, W. H. Press, and E. C. Turner, Annu. Rev. Astron. Astrophys. **30**, 499 (1992)
- [5] R. R. Caldwell, R. Dave, and P. J. Steinhardt, Phys. Rev. Lett. **80**, 1582 (1998)
- [6] L. Wang, and P. J. Steinhardt, Astrophys. J. **508**, 483 (1998); Z. Haiman, J. J. Mohr, and G. P. Holder, Astrophys. J. **553**, 545, (2001); J. Weller, R. A. Battye, and R. Kneissl, Phys. Rev. Lett. **88**, 231301 (2002)
- [7] C. Blake, and K. Glazebrook, Astrophys. J. **594**, 665 (2003); W. Hu, and Z. Haiman, Phys. Rev. D. **68**, 063004 (2003); A. Cooray, Mon. Not. R. Astron. Soc. **348**, 250 (2004); H. J. Seo, and D. J. Eisenstein, Astrophys. J. **633**, 575 (2005)
- [8] W. Hu, Astrophys. J. Lett. **522**, L21 (1999); D. Huterer, Phys. Rev. D **65**, 63001 (2001); M. Takada, and B. Jain, Mon. Not. R. Astron. Soc. **348**, 897 (2004); Y. S. Song, and L. Knox, Phys. Rev. D **70**, 063510 (2004)
- [9] D. Park, and J. Lee, Phys. Rev. Lett **98**, 081301 (2007)
- [10] S. F. Shandarin, J. V. Sheth, and V. Sahni, Mon. Not. R. Astron. Soc. **353**, 162 (2004); S. F. Shandarin, H. A. Feldman, K. Heitmann, and S. Habib, Mon. Not. R. Astron. Soc. **367**, 1629 (2006)
- [11] S. Basilakos, Astrophys. J. **590**, 636 (2003)
- [12] J. M. Bardeen, J. R. Bond, N. K. Kaiser, and A. S. Szalay, Astrophys. J. **304**, 15 (1986)
- [13] V. Springel *et al.*, Nature, **435**, 629 (2005). The Millennium Run halo catalogs are publicly available at <http://www.mpa-garching.mpg.de/millennium>
- [14] F. Hoyle, and M. S. Vogeley, Astrophys. J. **566**, 641 (2002)
- [15] M. Strauss *et al.*, Astrophys. J. **124**, 1810 (2002)